8-1-2014

Change In Depletion Curve Under Projected Climatic Scenarios For A Snow Covered Catchment In Arunachal Himalaya (India)

Arnab Bandyopadhyay

Aditi Bhadra

Tobom Rukbo

Sanayanbi Hodam

11th International Conference on Hydroinformatics
HIC 2014, New York City, USA

CHANGE IN DEPLETION CURVE UNDER PROJECTED CLIMATIC SCENARIOS FOR A SNOW COVERED CATCHMENT IN ARUNACHAL HIMALAYA (INDIA)

A BANDYOPADHYAY (1), A BHADRA (1), T RUKBO (2), SANAYANBI H (3)
(1): Assistant Professor, Department of Agricultural Engineering, North Eastern Regional Institute of Science and Technology, Nirjuli (Itanagar), Arunachal Pradesh 791109, India
(2): Post Graduate Student, Department of Agricultural Engineering, North Eastern Regional Institute of Science and Technology, Nirjuli (Itanagar), Arunachal Pradesh 791109, India
(3): Research Scholar, Department of Agricultural Engineering, North Eastern Regional Institute of Science and Technology, Nirjuli (Itanagar), Arunachal Pradesh 791109, India

Snow-cover depletion curve (SDC) is essential for snowmelt runoff modeling in any snow-dominated catchment. The present study deals with change in the SDC of Nuranang river basin of Arunachal Pradesh in future years under different projected climatic scenarios. Eleven years' meteorological data were used to normalize the temperature and precipitation data of the selected hydrological year (2007) so that the impact of their yearly fluctuations on the snow cover depletion is eliminated. The conventional depletion curve (CDC) representing present climate was derived by determining and interpolating the snow-covered area (SCA) percentages from cloud-free satellite images for year 2007 using NDSI model. The temperature and precipitation changes under different projected climatic scenarios (A1B, A2, B1, and IPCC Commitment) were obtained from https://gisclimatechange.ucar.edu/ for future years (2020, 2030, 2040, and 2050) and downscaled for the selected basin. Change in the cumulative snowmelt depth with respect to present climate for different future years were studied by degree-day approach and were found to be highest under A1B, followed by A2, B1, and IPCC Commitment scenarios. Assuming constant initial snow reserve on 1st February, dates of the snow-cover depletion curve were shifted backward based on the cumulative snowmelt depth corresponding to new climate. It was observed that the A1B climatic scenario affected the depletion pattern most making the depletion of snow to start and complete faster. Advancing of depletion curve for different future years was found to be highest under A1B and lowest under IPCC Commitment scenarios with A2 and B1 in-between them.

INTRODUCTION

In mountain basins, seasonal snow-cover extent and its accumulation and depletion patterns are changed due to change in climate. Hydrological models are now increasingly used for predicting the climate affected runoff. Snow-coverage is the main input variable for a wide variety of snowmelt runoff models. Martinec and Rango [1] employed a method to simulate the changed hydrological regime in mountain basins for any climatic change involving air

temperature and precipitation. Rango and Martinec [2] showed that in mountain snow basins, a change in climate will likely cause a change in the basin snow-cover extent.

Snow-cover depletion curve (SDC) indicates the snow-coverage on each day of the melt season and are commonly obtained by interpolating percentages of snow-covered area for dates when cloud-free satellite images are available. For snow-cover, a number of space borne sensors with various spectral, spatial, and temporal resolutions are available that satisfactorily fulfill the needs of climatologists and hydrologists.

Rango and Martinec [3] evaluated the average areal water equivalent of the seasonal snow-cover on 1 April in the basin of the Rio Grande at Del Norte, Colorado from periodical snow-cover mapping by LANDSAT. Gupta *et al.* [4] has chosen the River Beas, in northwest India, to study the relation between snow-cover area and snowmelt runoff. Seidel *et al.* [5] carried out seasonal and short-term runoff forecasts for two hydropower stations in the upper Rhine basin based on snow-cover monitoring by LANDSAT and SPOT. Seidel *et al.* [6] evaluated the combined influence of increased temperatures and changed precipitation on the seasonal snow-cover and runoff for the upper Rhine basin at Felsberg. König *et al.* [7] developed various methods for measuring snow and glacier ice properties with satellite remote sensing.

Singh and Bengtsson [8] studied the impact of three warming scenarios (T+1, T+2 and T+3 °C) and prepared more than 160 new snow-cover depletion curves for different elevation zones of a basin over a study period of nine years. Gupta *et al.* [9] showed that based on IRS-LISS-III sensor data it was possible to discriminate between dry snow and wet snow, the threshold NIR reflectance for such a discrimination being in the range of around 0.5.

Kulkarni *et al.* [10] showed that the normalized difference snow index (NDSI) value can be effectively used to map the aerial extent of snow-cover from AWiFS scenes if a threshold value of 0.4 is used to differentiate snow-covered areas from non-snow areas. Negi *et al.* [11] used a technique based on NDSI with vegetation information and NIR band reflectance for snow-cover distribution in the Beas basin. Sensoy *et al.* [12] found that the linear regressions between snow-cover area (SCA) and temperature resulted in high coefficient of determination (0.75-0.90). Jain *et al.* [13] found an exponential relationship between SCA and cumulative mean air temperature (CMAT). Akyurek *et al.* [14] developed a relationship between MODIS-derived SCA and CMAT for five elevation zones of the Upper-Euphrates basin.

Hall *et al.* [15] found out that percentage of basin-wide snow-cover and timing of snowmelt are primary drivers of discharge in the snow-dominated river basins. In mountainous areas, the runoff from snowmelt would be increased and redistributed during the snowmelt season as snowmelt patterns would be affected by changed climate.

The present study has been undertaken to derive conventional depletion curve for a selected hydrological year representing present climate and thereby regenerate climate-effected depletion curves under different projected climatic scenarios for future years.

STUDY AREA AND DATA ACQUISITION

Nuranang river basin (Fig. 1) with an area of 52 km^2, located in West Kameng district of Arunachal Pradesh, India, was selected as the study area. Nuranang River originates from Sela Lake at 4211 m AMSL and joins Tawang River as Nuranang falls at Jang. The outlet point of the basin lies at an elevation of 3474 m AMSL. Elevation of the basin ranges between 3143 m and 4946 m AMSL with an average slope of 51%. At upper elevation, climate is alpine and at lower elevation the basin experiences a temperate climate.

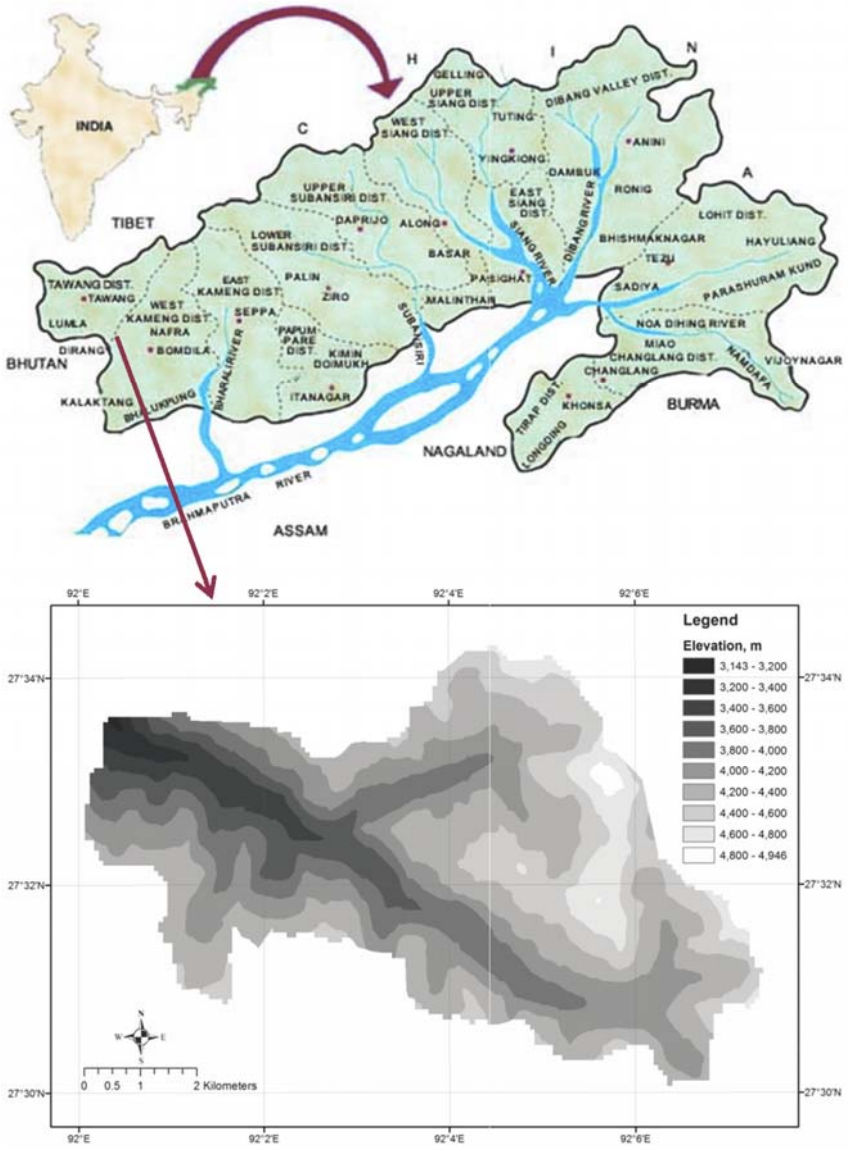

Figure 1. Nuranang river basin, Arunachal Pradesh, India

Monsoon season is spread over five months from May to September with average annual precipitation of 1,139 mm. The entire basin is dominated by seasonal snow which starts accumulating from October and continues till March. Melting of snow starts in February and gets completely depleted in June with some year-to-year variations.

Daily meteorological data for 11 years (2000-2010) were collected from Central Water Commission (CWC), Itanagar, Arunachal Pradesh, India. The 11-year (2000-2010) average temperature and precipitation data (Fig. 2) show that, in the month of February, the temperature is lowest and then increases till mid-August; while monthly cumulative precipitation attains peak in the month of July. Both of them have a great impact on the snow-cover depletion pattern.

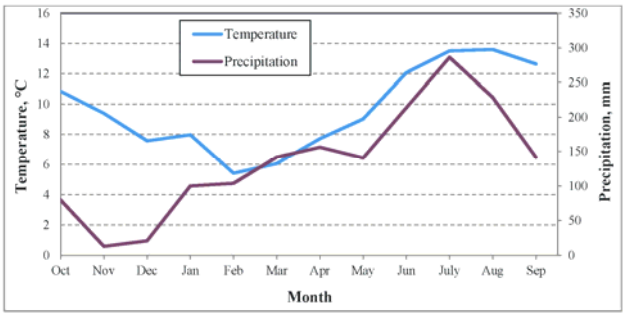

Figure 2. Average monthly mean temperature and monthly total precipitation

Satellite images (LISS-III/AWiFS) for snow accumulation and ablation period (October to June) were procured for the selected hydrological year 2007. The projected temperature and precipitation data were downloaded from National Center for Atmospheric Research (NCAR) website (https://gisclimatechange.ucar.edu/) for different climatic scenarios, i.e., A1B, A2, B1, and IPCC commitment. These data were downscaled and used to quantify the change in temperature and precipitation for future years 2020, 2030, 2040, and 2050 (Tables 1 and 2) with respect to the present climate for generating climate effected depletion curves under different climatic scenarios.

Degree-day factor (*a*) can be estimated from daily decrease in snow water equivalent (SWE) per degree increase in degree-days. Average of maximum and minimum temperatures of a particular day refers to degree-days (T) of that particular day. SWE of new snow is less and it increases as the snow pack ripens. As a result, degree-day factor increases with advancement of the melting season. Hence, different values for different months were assumed in this study as per WMO recommendation. Critical temperature, which decides whether the precipitation during the snowmelt season is snow or rain, was calibrated to be 1.0 °C in a snowmelt modeling study undertaken in the same Nuranang river basin. The near surface temperature lapse rate was taken as 0.5 °C/100 m following another study in the region. The SRTM DEM (90 m resolution) was downloaded from GLCF (http://glcf.umiacs.umd.edu/data/) for the study area. After filling the no-data pixels and delineating the basin boundary with respect to the selected outlet, the elevation range was found to vary between 3143 and 4946 m AMSL (Fig. 1).

METHODOLOGY

Snow cover mapping

SCA percentage is referred to as the areal extent of snow-covered ground which is usually expressed as percentage of total area in a basin. In the Himalayas, cloud cover is quite common. In the visible portion of the electromagnetic spectrum, snow and cloud, both appear bright white and create problem in snow-cover area estimation. Mountain shadow also makes it

Table 1. Change in temperature in °C

Scenarios	2020	2030	2040	2050
A1B	0.44	0.84	0.97	1.62
A2	0.27	0.69	0.50	1.18
B1	0.30	0.45	0.66	0.58
IPCC	0.25	0.26	0.13	-0.06

Table 2. Change in precipitation in %

Scenarios	2020	2030	2040	2050
A1B	6	-10	18	-7
A2	-14	-2	22	-3
B1	-12	-3	2	-4
IPCC	-4	-2	3	7

difficult to discriminate snow-covered areas under mountain shadow from snow free areas.

The NDSI is useful for identification of snow and separating it from clouds. NDSI uses the high and low reflectance of snow in visible (green) and shortwave infrared (SWIR) bands, respectively, and can delineate and map the snow in mountain shadows [16]. Additionally, the reflectance of clouds remains high in SWIR band, thus NDSI allows discrimination of clouds from snow. The NDSI was estimated from LISS-III/AWiFS data as [17]:

$$\text{NDSI} = [\text{Reflectance (B2)} - \text{Reflectance (B5)}]/ [\text{Reflectance (B2)} + \text{Reflectance (B5)}] \quad (1)$$

An NDSI model was developed in ERDAS Imagine for discrimination of snow and cloud from the LISS-III and AWiFS data of the study area based on the flowchart given by Kulkarni *et al.* [10]. Pixels with NDSI greater than 0.4 were marked as snow pixels and the rest of the basin was marked as no-snow. The SCA of the whole basin was determined in ArcGIS by masking the snow pixels with the basin boundary.

Development of climate-affected depletion curve

The conventional depletion curve (CDC) for the selected hydrological year was developed by generating smooth curves through discrete SCA% obtained from cloud-free dates and plotting these daily SCA% values against date. From the DEM of the whole basin, mean hypsometric elevation ($\bar{h}$) of the basin was found to be 4215 m. Temperature data, measured at the outlet, were adjusted by temperature lapse rate up to $\bar{h}$. The temperature and precipitation data for the selected hydrological year were normalized to represent the present climatic condition so that the impact of their yearly fluctuation on the snow-cover depletion is eliminated [18].

The decline of snow-cover extent not only depends on the initial snow reserve (which is assumed to be constant at the beginning of the melt season) but also on the climatic conditions of the year being considered because of changed amount and period of new snow falling during the snowmelt season. In this study, different projected climatic scenarios (A1B, A2, B1, and IPCC Commitment) were considered for future years of 2020, 2030, 2040, and 2050. The IPCC Special Report on Emissions Scenarios (SRES): Summary for Policymakers (https:// www.ipcc.ch/pdf/special-reports/spm/sres-en.pdf) describes these scenarios.

When the temperature at a particular day in the depletion period is lower than critical temperature (1.0 °C for the study area), the precipitation is considered as new snow and it contributes to snowmelt depth for the next day when temperature exceeds critical temperature. The snowmelt depth is calculated by multiplying the degree-days (T_{norm}) with degree-day factor (a) corresponding to next day. Climate affected depletion curve of snow-covered area for a changed climate takes into account the amount of new snowfall on a particular day during the melt season. In this study, it was attempted to derive the effect of climate change on the average depletion curve of the basin in the future years 2020, 2030, 2040, and 2050 under the four projected climatic scenarios (A1B, A2, B1, and IPCC Commitment). The shifting of dates for climate affected snow-cover depletion curves for 2020, 2030, 2040, and 2050 were determined following Rango and Martinec [2] and Martinec et al. [18] based on cumulative snowmelt depth. Climate affected depletion curves were generated by plotting the daily value of SCA% (from CDC) against these shifted dates.

RESULTS AND DISCUSSION

Change in cumulative snowmelt depth

Fig. 3 shows the cumulative snowmelt depth curves of the basin during ablation period under present climate and different projected climatic scenarios in future years. It can be observed that the cumulative snowmelt depth at the end of the ablation period (i.e., on 2nd June) is expected to increase from the present climatic condition under all projected climatic scenarios (except for IPCC Commitment in 2050). Change in the cumulative snowmelt depth for different future years is maximum under A1B and minimum under IPCC Commitment scenarios. Change corresponding to A2 and B1 is in-between A1B and IPCC Commitment scenarios.

Climate-affected depletion curves

The CDC for the basin along with climate affected depletion curves computed for different projected climatic scenarios in future years are shown in Fig. 4. It can be inferred that the A1B climatic scenario affects the snow-cover depletion most. As a result, the depletion of snow completes faster in this scenario. Climate affected depletion curve under IPCC commitment scenario almost matches the CDC for present climate. Climate affected depletion curves under A2 and B1 scenarios are in-between A1B and IPCC Commitment scenarios.

Compared to CDC, and assuming constant initial snow reserve (SCA 100%) on 1st February, the depletion starts from nine to 10 days earlier and completes from two to 14 days earlier under A1B scenario resulting a the ablation period duration varying between 99 and 112 days in future years (2020, 2030,2040, and 2050). Under A2 scenario, the start date shifts backward by nine to 10 days and the end date shifts backward by two to nine days with snowmelt duration varying from 104 to 112 days. Under B1 scenario, the backward shifting of start date is found to be 10 days on all years and the backward shifting of end date varies from two to four days making the ablation period varying from 110 to 112 days. Under IPCC Commitment scenario, depletion starts from 10 days earlier to four days delayed and completes from one day earlier to one day delayed with duration of snowmelt period varying from 101 to 114 days. It was also observed that shift of ending date of the snow-cover depletion was very

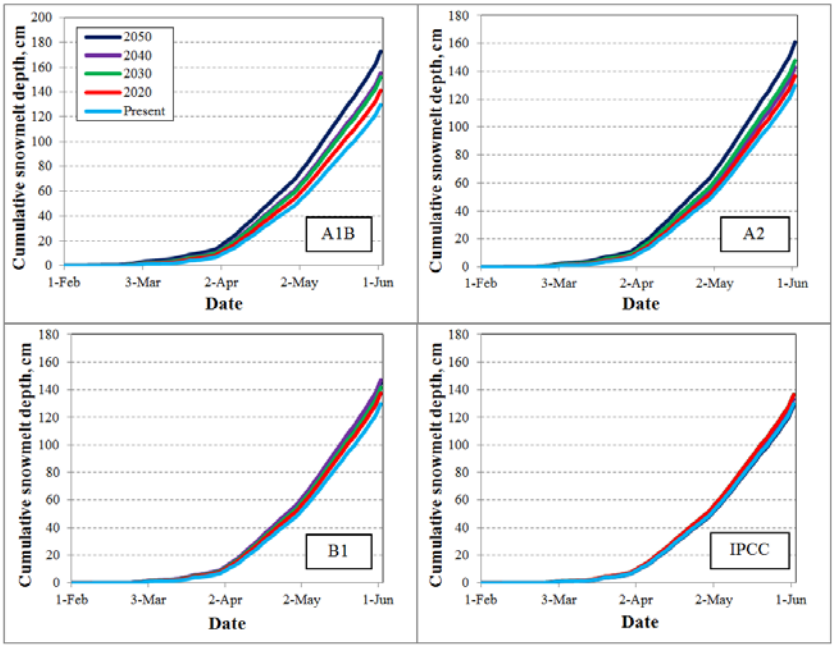

Figure 3. Cumulative snowmelt depths for future years under different scenarios

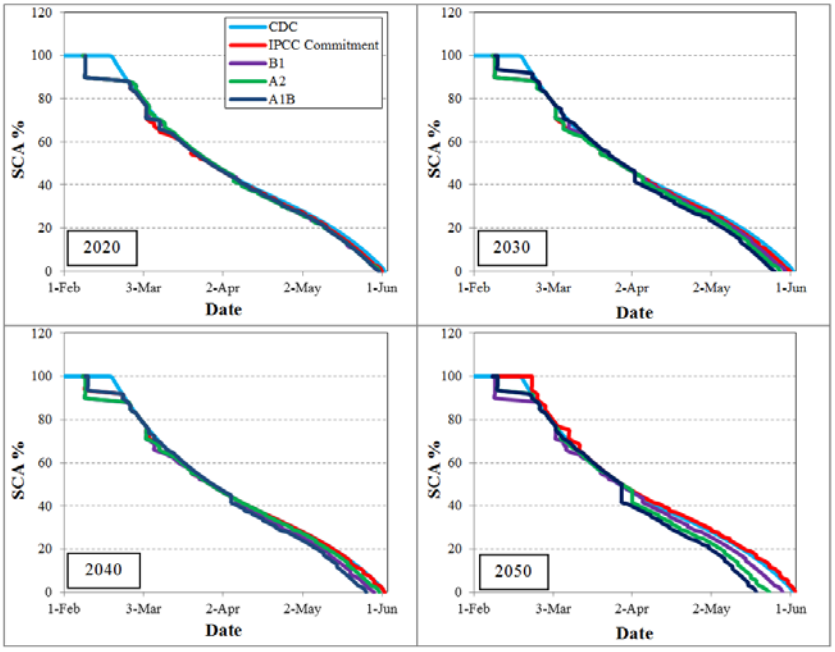

Figure 4. Cumulative snowmelt depths for future years under different scenarios

similar with change in temperature in all future years and under all projected climatic scenarios. For any future year, backward shift in ending date of snow depletion is highest under A1B and lowest under IPCC Commitment scenarios, with A2 and B1 in-between them.

CONCLUSIONS

Snow-cover depletion starts in the month of February in the selected eastern Himalayan basin. Change in the cumulative snowmelt depth is found to be maximum under A1B and minimum under IPCC Commitment scenarios. The change in the cumulative snowmelt depth follows the same trend as temperature with respect to present climatic condition under all projected scenarios. Assuming constant initial snow reserve on 1st February, and excluding IPCC Commitment scenario in 2050, depletion is found to start from nine to 10 days earlier and complete from one to 14 days earlier compared to present climate. This shift of ending date of the snow-cover depletion is found to be following a matching trend with change in temperature over future years under different projected climatic scenarios. The duration of ablation period is found to be varying between 99 and 114 days compared to 103 days at present. In a nutshell, the entire depletion curve is found to be shifted backward without much change in its shape. This advancing of depletion curve for different future years is highest under A1B and lowest under IPCC Commitment scenarios, with A2 and B1 in-between them.

REFERENCES

[1] Martinec J. and Rango A., “Effects of climate change on snowmelts runoff patterns”, *Proc. Remote sensing and large scale global processes*, Baltimore, IAHS Publ. no. 186, (1989), pp 31-38.

[2] Rango A. and Martinec J., “Areal extent of seasonal snow-cover in a changed climate”, *Nordic Hydrol.*, Vol. 25, (1994), pp 233-246.
[3] Rango A. and Martinec J., “Water storage in mountain basins from satellite snow-cover mapping”, In: Baumgartner M.F., Schultz G.A. and Johnson A.I. (Eds.). *Remote Sensing and Geographical Information Systems for Design and Operation for Water Resources System*, IAHS Publ. no. 242, (1997), pp 83-91.
[4] Gupta R.P., Duggal A.J., Rao S.N., Sankar G. and Singhal B.B.S., “Snow-cover area vs. snowmelt runoff relation and its dependence on geomorphology – A study from the Beas catchment (Himalayas, India)”, *J. Hydrol.*, Vol. 58, No. 3-4, (1982), pp 325-339.
[5] Seidel K., Brusch W. and Steinmeier C., “Experiences from real time runoff forecasts by snow-cover remote sensing”, *Proc. IGARSS, surface and atmospheric remote sensing: technologies, data analysis and interpretation*, IEEE, Vol. 4, (1994), pp 2090-2093.
[6] Seidel K., Ehrler C. and Martinec J., “Effects of climate change on water resources and runoff in an alpine basin”, *Hydrol. Process.*, Vol. 12, No. 10-11, (1998), pp 1659-1669.
[7] König M., Winther J-G. and Isaksson E., “Measuring snow and glacier ice properties from satellite”, *Reviews of Geophysics*, Vol. 39, No. 1, (2001), pp 1-27.
[8] Singh P. and Bengtsson L. “Effect of warmer climate on the depletion of snow-covered area in the Satluj basin in the western Himalayan region”, *Hydrol. Sci. J.*, Vol. 48, No. 3, (2003), pp 413-425.
[9] Gupta R.P., Haritashya U.K. and Singh P., “Mapping dry/wet snow-cover in the Indian Himalayas using IRS imagery”, *Rem. Sens. Environ.*, Vol. 97, No. 4, (2005), pp 458-469.
[10] Kulkarni A.V., Singh S.K., Mathur P. and Mishra V.D., “Algorithm to monitor snow-cover using AWIFS data of RESOURCESAT-1 for the Himalayan region”, *Int. J. Remote Sens.*, Vol. 27, No. 12, (2006), pp 2449-2457.
[11] Negi H.S., Kulkarani A.V. and Semwal B.S., “Estimation of snow-cover distribution in Beas basin, Indian Himalaya using satellite data and ground measurement”, *J. Earth Syst. Sci.*, Vol. 118, No. 5, (2009), pp 525-538.
[12] Sensoy A., Uysal G., Sorman A.A. and Sorman A.U., “Topographic effects on snow depletion curves of upper Euphrates river basin, Turkey”, *Proc. Water observation and informations Systems*, Ohrid, (2010), pp 25-29.
[13] Jain S.K., Thakural L.N., Singh R.D., Lohani A.K. and Mishra S.K., “Snow-cover depletion under changed climate with the help of remote sensing and temperature data”, *Nat. Hazards*, Vol. 58, (2011), pp 891-904.
[14] Akyurek Z., Surer S. and Bolat K., “Temporal analysis of snow-cover depletion in the eastern part of Turkey based on MODIS-Terra and temperature data”, *Geophysical Research Abstracts*, Vol. 14, (2012), pp 8226.
[15] Hall D.K., Foster J.L., DiGirolamo N.E. and Riggs G.A. “Snow-cover, snowmelt timing and stream power in the Wind River Range, Wyoming”, *Geomorphology*, Vol. 137, No. 1, (2012), pp 87-93.
[16] Kulkarni A.V., Srinivasulu J., Manjul S.S. and Mathur P., “Field based spectral reflectance studies to develop NDSI method for snow-cover monitoring”, *J. Indian Society of Remote Sens.*, Vol. 30, No. 1&2, (2002), pp 73-80.
[17] Hall D.K., Riggs G.A., Salomonson V.V., Digirolamo D.G. and Bayr K.J., “MODIS snow-cover products”, *Remote Sens. Environ.*, Vol. 83, (2002), pp 181-194.
[18] Martinec J., Rango A. and Roberts R., “*Snowmelt-Runoff Model (SRM) user’s manual*”, USDA Jornada Experimental Range, New Mexico State University, Las Cruces, NM 88003, USA, (2007).